



Fermi National Accelerator Laboratory

FERMILAB-Conf-96/136

**Optimization of the LHC Interaction Region with Respect to
Beam-Induced Energy Deposition**

N.V. Mokhov and J.B. Strait

*Fermi National Accelerator Laboratory
P.O. Box 500, Batavia, Illinois 60510*

June 1996

Presented at the *European Particle Accelerator Conference*,
Barcelona, Spain, June 10-14, 1996

Disclaimer

This report was prepared as an account of work sponsored by an agency of the United States Government. Neither the United States Government nor any agency thereof, nor any of their employees, makes any warranty, expressed or implied, or assumes any legal liability or responsibility for the accuracy, completeness, or usefulness of any information, apparatus, product, or process disclosed, or represents that its use would not infringe privately owned rights. Reference herein to any specific commercial product, process, or service by trade name, trademark, manufacturer, or otherwise, does not necessarily constitute or imply its endorsement, recommendation, or favoring by the United States Government or any agency thereof. The views and opinions of authors expressed herein do not necessarily state or reflect those of the United States Government or any agency thereof.

Optimization of the LHC Interaction Region with Respect to Beam-Induced Energy Deposition*

N. V. Mokhov and J. B. Strait[†]

Fermi National Accelerator Laboratory

P.O. Box 500, Batavia, Illinois 60510

[†] *On leave at CERN, CH-1211 Geneva, Switzerland*

June 10, 1996

Abstract

Energy deposition in the superconducting magnets by particles from p-p collisions is a significant challenge for the design of the LHC high luminosity insertions. We have studied the dependence of the energy deposition on the apertures and strengths of insertion magnets and on the placement of absorbers in front of and within the quadrupoles. Monte Carlo simulations were made using the code DTUJET to generate 7x7 TeV p-p events and the code MARS to follow hadronic and electromagnetic cascades induced in the insertion components. The 3D geometry and magnetic field descriptions of the LHC-4.1 lattice were used. With a quadrupole coil aperture ≥ 70 mm, absorbers can be placed within the magnet bore which reduce the peak power density, at full luminosity, below 0.5 mW/g, a level that should allow the magnets to operate at their design field. The total heat load can be removed by a cooling system similar to that used in the main magnets.

*Presented at the *European Particle Accelerator Conference*, Barcelona, Spain, June 10-14, 1996

Figure 1: The LHC low- β insertions including absorbers which reach the 10σ limit (injection/collision optics: solid/dashed line) for $d_{\text{coil}}=70$ mm quadrupoles.

2 Computer Modelling

Fig. 1 shows the LHC low- β insertion [1, 6]. The inner triplet is made of four identical high-gradient quadrupoles with coil inner diameter $d_{\text{coil}}=70$ mm [7] (Q1 and Q3 focusing and Q2a and Q2b defocusing), which are powered in series and operate at a maximum gradient of 227 T/m at the high luminosity IRs. Two independently powered “trim” quadrupoles of $d_{\text{coil}}=85$ mm and maximum operating gradient of 120 T/m (Q01 and Q03) provide the additional strength required by Q1 and Q3 and allow tuning of the triplet. Behind the triplet are the dipoles D1 (single aperture) and D2 (twin aperture). They have $d_{\text{coil}}=85$ mm and an operating field of 4.3 T. Their length (11.5 m) is set by the required strength at the combined experimental and injection insertions (points 2 and 8), where space is more limited than at the high luminosity IRs (points 1 and 5).

Alternate IR designs with quadrupoles of $d_{\text{coil}}=60$ mm and 80 mm have also been considered. The gradients were scaled with d_{coil} (a little more slowly than $1/r$ for thick shell quadrupoles) and corresponding length changes were made. Optics with minimal perturbations to the baseline were computed for injection (450 GeV, $\beta^*=6$ m) and collision (7 TeV, $\beta^*=0.5$ m) conditions and are summarized in Table 1. Relative to the baseline 70 mm case β_{max} for 80 (60) mm quadrupoles changes by +6.6% (-5.1%) yielding changes in the maximum beam size of +3.3% (-2.6%), considerably less than the change in d_{coil} . Thus increasing the aperture should improve the field quality over the region occupied by the beam and allow more shielding inside the magnet bore, while decreasing the aperture will have the opposite effect.

A 1.8 m long copper absorber is placed in front of the triplet and stainless steel absorbers are placed within the magnet bores to minimize the energy deposition in the coils. The LHC design requires [1] that the physical aperture, including effects of dispersion, closed orbit errors, construction and alignment tolerances, and the crossing angle in the IRs be everywhere at least 10σ (except at the beam cleaning collimators), where σ is the *rms* beam size. Fig. 1 shows the 10σ limit for injection and

Table 1: Characteristics of the IR optics.

d_{coil}	60 mm		70 mm		80 mm	
L_{mag}	5.1 m		5.5 m		6.0 m	
Stage	Coll.	Inj.	Coll.	Inj.	Coll.	Inj.
G (T/m)						
Q1-Q3	251	15.5	227	14.0	202	12.4
Q01	70	4.7	80	5.3	92	6.1
Q03	105	8.5	101	7.7	95	6.1
β_{max} (m)	4204	358	4431	377	4724	402

Table 2: Minimum inner radii of absorbers.

d_{coil}	60 mm	70 mm		80 mm
Clearance	10σ	10σ	8σ	10σ
Collimator	14.0	14.0	12.0	14.0
Q1	19.0	19.5	17.0	20.0
Q01	21.5	21.5	18.5	22.0
Q2-Q03	26.5	27.0	23.5	28.0
D1	36.5	37.5	34.0	38.0

collision conditions and absorbers with inner radius r_{in} at this limit. The cusp between Q2b and Q3 is where the maximum β changes from one plane to the other. The outer radius of the internal absorbers is 2 mm less than r_{coil} . Table 2 gives r_{in} of the absorbers for the three quadrupole diameters. To allow the effectiveness of the absorber to be evaluated versus thickness for a fixed insertion design, the r_{in} for 8σ are given for the 70 mm quadrupoles. As the r_{coil} grows from 30 to 40 mm the 10σ limits increase by only 0.5 mm (Q1-Q01) and 1.5 mm (Q2-Q03), allowing an increased absorber thickness. However, the D1 absorber decreases from 5.5 to 4 mm thick.

The p-p collisions and showers in the IR components are simulated with the DTUJET93 event generator [8] and the MARS code [9], version 13(96) respectively. Charged particles are tracked through the lattice and the fields within each magnetic element. The cut-off energies are 1 MeV (charged particles), 0.2 MeV (photons) and 0.5 eV (neutrons). Magnet coils are modeled with 4 radial bins of 8.5 mm depth, azimuthal bins varying from 5° at the horizontal and vertical planes to 15° between, and axial bins between 1.1 m (Q1) and 3.8 m (D1) long. The magnet coils, which are a mixture of NbTi, copper, insulation and helium, are simulated as a homogeneous material with $A=50$, $Z=23$ and $\rho=7$ g/cm³. Details such as cooling channels in the yoke and coil ends are not included. Statistical errors on the Monte Carlo calculation are estimated to be $\pm 15\%$ for P_{max} , $\pm 6\%$ for the energy deposited in each magnet, and $\pm 1\%$ for the total power in the inner triplet, based on comparison of results from different runs with independent random seeds.

3 Results

Fig. 2 shows P_{max} vs z for the IR with 70 mm quadrupoles and no internal absorbers, absorbers at 10σ and 8σ , and all quadrupole absorbers of a uniform radius at the 10σ limit in Q2-Q03. The front absorber aperture is set at 10σ for the case of no internal absorbers. With no internal absorber $P_{\text{max}} = 1.2 \pm 0.2$ mW/g, at or above the allowable limit. With individually sized 10σ absorbers the peak is a factor of 3

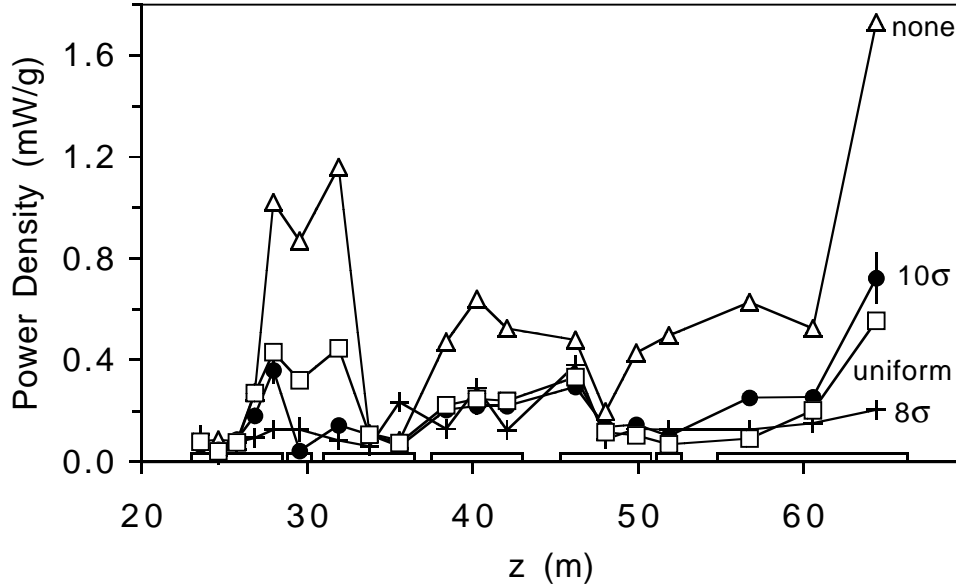


Figure 2: P_{max} vs z for 70 mm quadrupoles with several absorber configurations.

smaller, giving a reasonable safety margin. Use of an 8σ absorber reduces P_{max} in Q1, but there is little overall improvement. Increasing r_{in} of the absorbers in Q1-Q01 to match the other quadrupoles results in a 25% increase in P_{max} . However, this increase may not be statistically significant and further study will be required to determine if it is necessary to use different absorbers in Q1 and Q01 than in the rest of the triplet.

An unacceptably large P_{max} is observed at the back of D1 even with a 10σ absorber. However, at the high luminosity IRs it is possible to move the outer dipole D2 up to an additional 90 m farther from D1. This would reduce the length of D1 to one-third its present value, corresponding to the first bin in Fig. 2, which has an acceptable power density. Alternatively the integrated strength would be low enough to allow use of conventional magnets for D1 and D2, eliminating the problem altogether.

The cases of three quadrupole diameters with 10σ absorbers are compared in Fig. 3. P_{max} is 40% larger (30% smaller) with 60 mm (80 mm) quadrupoles than the baseline 70 mm case. The reduced margin with $d_{coil}=60$ mm makes this option unattractive. The 80 mm case has a significantly larger margin, which could be used, if required, to provide additional physical aperture. The larger β_{max} is unlikely to be a problem since the field quality in the region occupied by the beam would be better with a larger aperture magnet.

Shown also is the case in which all quadrupoles, including Q01 and Q03, have the same $d_{coil}=70$ mm and the absorbers have a uniform r_{in} . P_{max} is 80% larger than

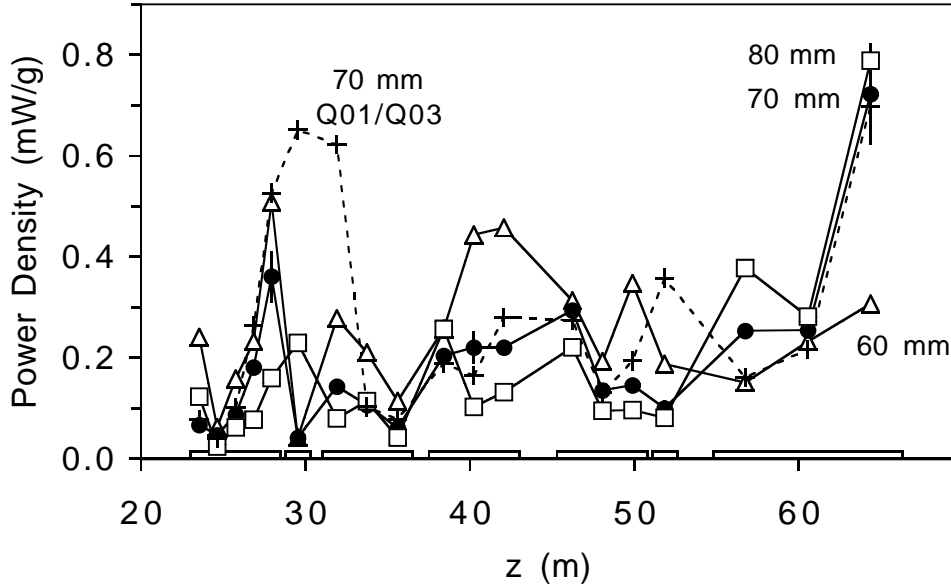


Figure 3: P_{max} vs z for main quadrupoles of three d_{coil} with 85 mm trim quadrupoles, and 70 mm main with 70 mm trim quadrupoles. The data are plotted at the z values for the 70 mm quadrupoles to ease comparison.

the case with 85 mm trims and individually sized absorbers (Fig. 3) and 45% larger than with uniform absorbers (Fig. 2). Apparently it is unacceptable to have a continuous annular gap between the absorber outer and coil inner radii.

Table 3 summarizes the total power deposited in the magnets and internal absorbers. The quadrupoles and the dipole D1 are considered separately, since the actual dipole configuration will probably be different than that considered here. There

Table 3: Total deposited power (W).

d_{coil} (mm)	70	70	70	70	60	80
Absorber (σ)	none	10	10 unif	8	10	10
Quadrupoles	115	82	86	66	98	69
Absorbers	–	61	52	73	37	78
Total	115	143	138	139	135	147
D1	45	26	34	19	24	25
Absorber	–	10	16	15	12	9
Total	45	36	50	34	36	34

Table 4: Total power (W) deposited in each magnet for 70 mm quadrupoles with 10σ absorbers.

	Q1	Q01	Q2a	Q2b	Q3	Q03
Magnet	15	6	13	17	26	4
Absorber	18	10	5	9	13	7
Total	33	16	18	26	39	11

is little difference among the cases with internal absorbers. Up to half the power is deposited in the absorbers, and it is tempting to consider cooling them at a higher temperature. However, the insulating space between the absorber and the vacuum pipe would reduce the absorber thickness, making this option impractical except possibly with 80 mm magnets. The longitudinal power distribution is shown in Table 4 for 70 mm quadrupoles with 10σ absorbers. Averaged over each element, the power density varies from 3 W/m (Q2a) to 10 W/m (Q01). However, the variation within one magnet can be as large as a factor of 8 (Q1 with uniform diameter absorbers).

4 Conclusions

Energy deposited in the superconducting magnets is an important issue in the overall design of the LHC IRs. Reducing P_{max} to an acceptable level requires the use of internal absorbers at least 5-6 mm thick. Quadrupoles with $d_{coil}=70$ mm, the current baseline design, are large enough to accommodate such liners and leave a 10σ physical aperture. A larger d_{coil} would allow use of a thicker absorber, greater physical aperture for the same absorber thickness, or possibly cooling the absorber at a higher temperature than the magnet. P_{max} in D1 at the high luminosity IRs is unacceptably large if dipoles of the baseline length are used. However, here the dipoles can be moved farther apart reducing their length by up to a factor of 3 or allowing the use of conventional magnets.

5 Acknowledgements

We would like to thank P. Limon, R. Ostojic, K. Potter and T. Taylor for useful discussions. This work was supported in part by the U.S. Department of Energy.

References

- [1] “The Large Hadron Collider Conceptual Design,” CERN/AC/95-05(LHC), 1995, P. Lefèvre and T. Pettersson, editors.
- [2] K. Eggert and A. Morsch, “Particle Losses in the LHC Interaction Regions,” CERN AT/93-17 (DI), 1993; A. Morsch, “Local Power Distribution from Particle Losses in the LHC Inner Triplet Magnet Q1,” CERN AT/94-06 (DI), 1994.
- [3] A. Morsch, R. Ostojic, T.M. Taylor, “Progress in the Systems Design of the Inner Triplet of 70 mm Aperture Quadrupoles for the LHC Low-beta Insertions,” Proc. 4th European Part. Accel. Conf., London, England, 1994.
- [4] N. V. Mokhov, “Accelerator/Experiment Interface at Hadron Colliders: Energy Deposition in the IR Components and Machine Related Background to Detectors”, Fermilab-Pub-94/085, 1994.
- [5] L. Burnod, et al., “Thermal Modelling of the LHC Dipoles Functioning in Superfluid Helium,” Proc. 4th European Part. Accel. Conf., London, England, 1994.
- [6] R. Ostojic and T.M. Taylor, “Proposal for and Improved Optical and Systems Design of the LHC Low- β Triplets,” CERN AT/94-38 (MA), 1994.
- [7] R. Ostojic, T.M. Taylor and G.A. Kirby, “Design and Construction of a One-Metre Model of the 70 mm Aperture Quadrupole for the LHC Low- β Insertions,” Proc. 13th Int. Conf. on Mag. Tech. (MT13), Victoria, Canada, 1993.
- [8] P. Aurenche, et al., “DTUJET93”, Comput. Phys. Commun., **83**, p. 107, 1994.
- [9] N. V. Mokhov, “The MARS Code System User’s Guide, Version 13(95)”, Fermilab-FN-628, 1995.